Two-Dimensional Simulation of Inductive Plasma Sources with Self-Consistent Power Deposition

Ming Li, Han-Ming Wu, and Yunming Chen

Abstract—**A time averaged two-dimensional fluid model including an electromagnetic module with self-consistent power deposition was developed to simulate the transport of a low pressure radio frequency inductively coupled plasma source. Comparsions with experiment and previous simulation results show that the fluid model is feasible in a certain range of gas pressure. In addition, the effects of gas pressure and power input have been discussed.**

I. Introduction

A NUMBER of new high density plasma sources have been investigated recently, including electron cyclotron resonance (ECR) discharge, helical resonator discharge, helicon wave discharge, as well as inductively coupled plasma (ICP or TCP) discharge [1], [2]. In addition, considerable progress has been made in their applications [3]–[7]. These high density plasma sources can supply high ion fluxes to surfaces in etching or film deposition processes at low neutral gas pressure (1–20 mTorr), with controllable and directional ion energy. Sheath potentials in these discharges are relatively low, and the sheathes are thin. This results in collisionless ion motion through the sheathes.

The ICP source, as one type of high density plasma source, has been intensively studied both experimentally and theoretically. The ion energy, electron energy distribution function (EEDF) and the electric field have been measured by Fabry-Perot interferometry, and Langmuir probe, respectively [8]–[13]. The global model proposed in [1] was used to estimate the average plasma characteristics such as the plasma density, the plasma potential, electron temperature, etc. [14], [15]. In addition, two-dimensional numerical simulations of high density ICP sources have been carried out recently [15]–[17]. In [15], a fluid model was developed to study the Ar plasma transport with assumed power deposition profiles, results were compared with the results obtained with a global model over a wide range of pressure and power level (1–20 mTorr, 100–1000 W). References [16], [17] developed a hybrid model consisting of electromagnetic, electron Monte Carlo, and hydrodynamic modules. Based on this model, the plasma density, plasma potential, and ion fluxes for Ar, $O_2, Ar/CF_4/O_2$ gas mixtures have been studied.

In the present paper, a time averaged two-dimensional (r, x) ICP fluid model, including the inductive electromagnetic equations and self-consistent plasma power deposition profile, has been developed to study the argon plasma transport. The results agree quantitatively with those of experiments and other simulations.

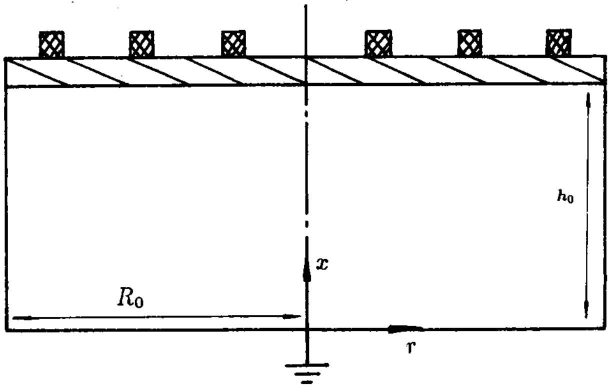

Fig. 1. Sketch of the inductively coupled plasma source.

II. Model Formulation

A typical ICP reactor is schematically shown in Fig. 1. The reactor is a squat metallic cylindrical chamber with a dielectric roof. A flat spiral inductive coil through which a radio frequency current (13.56 MHz) flows is placed on the top of the chamber. The plasma is generated and heated by an inductively coupled azimuthal electric field. Optional multipole magnets can also be placed around the outer periphery, whose effect is to smooth the plasma density in the radial direction and to increase the plasma density. The basic assumptions of the model are:

1) the effects of gas flow is negligible,
2) the EEDF is Maxwellian,
3) the ion temperature is assumed equal to the neutral temperature,
4) ion inertia is neglected,
5) the flat spiral inductive coil is simplified as three coaxial flat circular coils,
6) the neutral density and temperature are uniform.

A. Electromagnetic Equations

In the ICP reactor, the electromagnetic field can be primarily divided in two parts, one is the inductively coupled electromagnetic field $\boldsymbol{E_I}$, the other is the plasma static electric field $\boldsymbol{E_S}$. Fortunately, we can treat them seprately because the electromagnetic equations can be summed up and their results can be written as $\boldsymbol{E} = \boldsymbol{E_I} + \boldsymbol{E_S}$.

Manuscript received September 26, 1994; revised March 17, 1995. This work was supported in part by the National Natural Science Foundation of China, The Foundation of National Education Committee of China.

The authors are with the Institute of Mechanics, Chinese Academy of Sciences, Beijing 100080, China.

IEEE Log Number 9412960.

For the static electric field, the static electric potential (plasma potential) can be determined by the following equation:

$$\nabla^2\phi = \frac{e}{\varepsilon_0}(n_e - n_i) \tag{1}$$

where e is the elementary charge, ε_0 is permitivity, n_i, n_e are the ion and electron density, respectively. The static electric field $\boldsymbol{E}_S = -\nabla\phi$.

For the inductive electromagnetic field, according to assumption (5), $\boldsymbol{E}_I$ has the azimuthal component $E_{I\theta}$ only. Similar to [18], [19], if the oscillating current flows through the coil is $I = I_0 \cos \omega t$, the corresponding inductive electric field $E_{I\theta} = E_{I_1} \cos \omega t + E_{I_2} \sin \omega t$ should satisfy (2) and (3)

$$\nabla^2 E_{I_1} - E_{I_1}/r^2 - \xi\sigma\omega E_{I_2} = 0 \tag{2}$$

$$\nabla^2 E_{I_2} - E_{I_2}/r^2 + \xi\sigma\omega E_{I_1} = 0 \tag{3}$$

where $\xi = 4\pi\times 10^{-7} H/m, \sigma = n_e e^2/m_e\nu_{eN}[1+(\omega/\nu_{eN})^2]$ is the plasma electric conductivity. ν_{eN} is the collision frequency of electron-neutral. For the ICP reactor as shown in Fig. 1, on the metallic chamber wall and the reactor axis, $E_{I\theta} = 0$, while on the top surface, $E_{I\theta}$ is determined by the current I_0 in the coil and the inductive current $\sigma_{ij}E_{Ii,j}\Delta x_i \Delta r_j$ in the plasma. That is

$$E_{I_1} = -\frac{\xi\omega}{2\pi}\sum_{i,j}\left[\sqrt{\frac{r_j}{r_B}}H(k_{ij})\sigma_{ij}E_{I_2}\Delta x_i\Delta r_j\right] \tag{4}$$

$$\begin{aligned} E_{I_2} &= \frac{\xi\omega}{2\pi}I_0\sum_{n}\left[\sqrt{\frac{r_n}{r_B}}H(k_n)\right] \\ &\quad + \frac{\xi\omega}{2\pi}\sum_{i,j}\left[\sqrt{\frac{r_j}{r_B}}H(k_{ij})\sigma_{ij}E_{I_1}\Delta x_i\Delta r_j\right] \end{aligned} \tag{5}$$

where

$$\begin{aligned} H(k) &= \frac{2}{k}(F(k) - E(k)) - kF(k) \\ k_{i,j} &= 2\sqrt{r_B r_j/[(x_B - x_i)^2 + (r_B + r_j)^2]} \\ k_n &= 2\sqrt{r_B r_n/[(x_B - x_n)^2 + (r_B + r_n)^2]} \end{aligned}$$

where $F(k)$ and $E(k)$ are the complete elliptic integrals of the first and second kinds, (x_B, r_B) is the coordinates of the boundary points on the top surface, (x_n, r_n), is the coordinates of the nth excitation current loop, (x_i, r_j) is the coordinates of the (i, j)th grid.

B. Fluid Dynamic Equations

The time average equations for electrons and ions are

$$\nabla \cdot \boldsymbol{J_e} = R_i \tag{6}$$

$$\nabla \cdot \boldsymbol{J_i} = R_i \tag{7}$$

$$\nabla \cdot \boldsymbol{Q_e} = q_J - \sum_k R_k \epsilon_k e \tag{8}$$

where

$$\begin{aligned} \boldsymbol{J_e} &= -\mu_e n_e \boldsymbol{E}_S - \frac{k}{m_e\nu_{eN}}\nabla(n_e T_e) \\ \boldsymbol{J_i} &= \mu_i n_i \boldsymbol{E}_S - \frac{2k}{m_i\nu_{iN}}\nabla(n_i T_i) \\ \boldsymbol{Q_e} &= \frac{5}{2}kT_e\boldsymbol{J_e} - \frac{5}{2}\frac{k^2}{m_e\nu_{eN}}n_e T_e\nabla T_e \\ \mu_e &= \frac{e}{m_e\nu_{eN}}, \quad \mu_i = \frac{2e}{m_i\nu_{iN}} \end{aligned}$$

k is Boltzmann constant, m is mass, n is number density, T is temperature, $\boldsymbol{J}, \boldsymbol{Q}$ are the fluxes of charged particles and energy fluxes, subscript $\alpha(\alpha = e, i)$ denotes the electrons and ions. μ_e, μ_i are the electron and ion mobility, $\nu_{\alpha N}$ are the collision frequency of electron- and ion neutral.

The ionization rate R_i can be calculated by considering only the electron-impact ionization of ground state argon atoms $R_i = K_i n_e n_a$. The ionization rate coefficient K_i is expressed as follows:

$$K_i = \sigma_i \overline{V}_e \exp\left[-e\epsilon_i/kT_e\right]. \tag{9}$$

For other inelastic collisions between electrons and neutral atoms (excitation to resonance levels, excitation to metastable levels), the collision rate R_k, can be expressed as $R_k = K_k n_e n_a$, where

$$K_k = \sigma_k \overline{V}_e \exp\left[-e\epsilon_k/kT_e\right] \tag{10}$$

where $\overline{V}_e = \sqrt{8kT_e/\pi m_e}$ is the electron mean thermal speed. The constants σ_k, ϵ_k adopted in (4)–(8) are the same as in [5], [15].

In (6), q_J is the Joule heat absorbed by the plasma, which is the mean value over an RF cycle

$$q_J = \frac{1}{T}\int_0^T \sigma E^2\, dt = \sigma\left[\frac{1}{2}(E_{I_1}^2 + E_{I_2}^2)\right]. \tag{11}$$

The total input power is

$$P_t = 2\pi\int_0^{R_0}\int_0^{h_0} q_J r\, dr\, dx. \tag{12}$$

III. RESULTS AND DISCUSSIONS

The model described above was used to simulate an argon discharge over the range of pressure 10–20 mTorr and power 200–800 W. In the present simulation, the ICP reactor diameter is $2R_0 = 20$ cm, height is 7.5 cm, the minimum radius of the coil is 2.5 cm and the maximum is 8.5 cm.

The boundary conditions adopted in the present model are as follows: For n_e, n_i and ϕ, on the metallic wall $n_e = \phi = 0, (\nabla n_i)_\perp = 0$; on the axis $\partial n_e/\partial r = \partial n_i/\partial r = \partial\phi/\partial r = 0$; on the insulated top wall, the analytical results based on the thin plasma sheath was adopted [5]

$$\begin{aligned} J_{ew} &= \frac{1}{4}n_{es}\overline{V}_{es} \exp\left[-\frac{e\Delta\phi}{kT_{es}}\right] \\ J_{iw} &= n_{is}V_i \\ \phi_w &= \phi_s + \frac{kT_{es}}{e} \ln\left[\frac{4J_{iw}}{n_{es}\overline{V}_{es}}\right] \end{aligned}$$

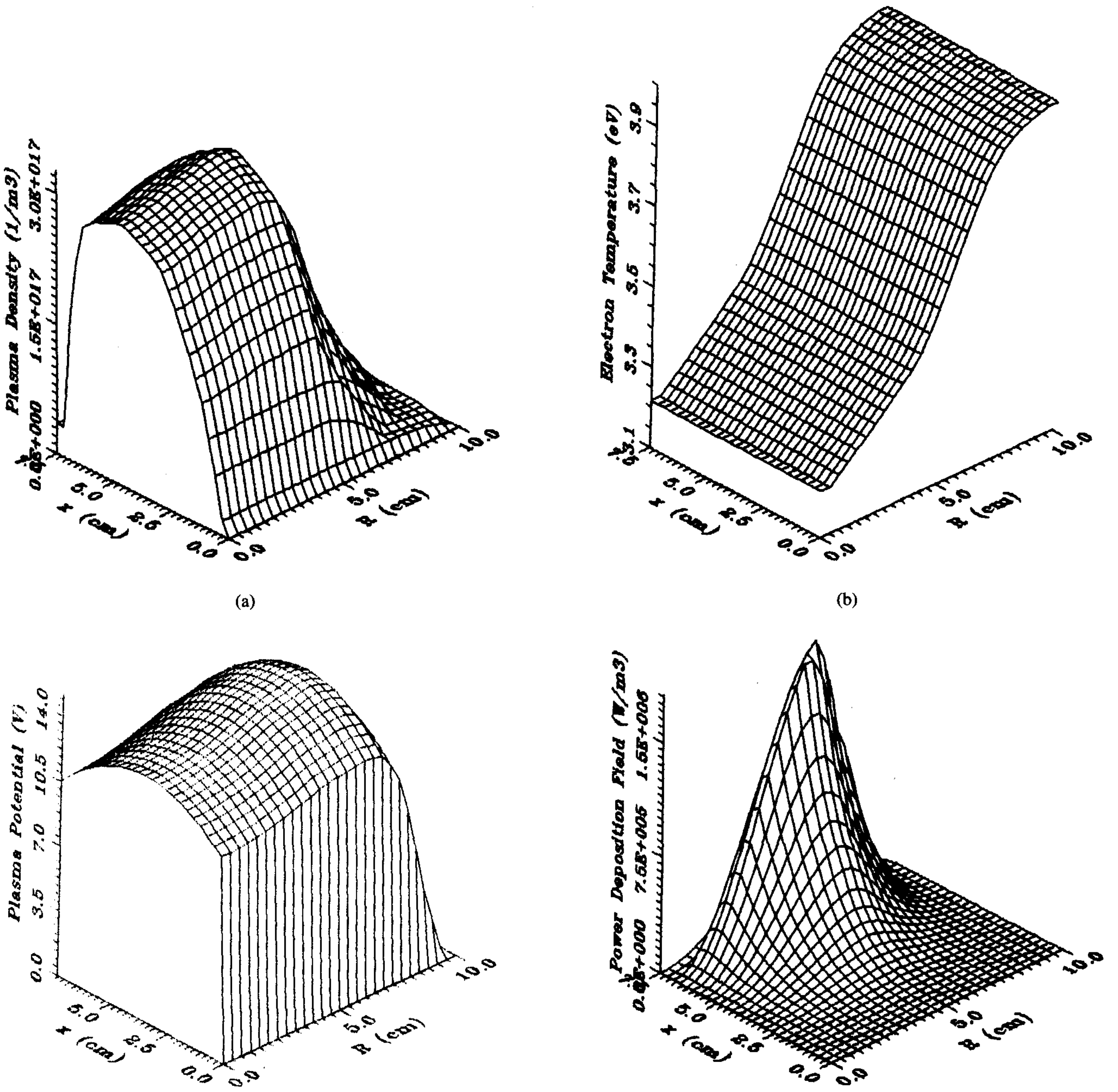

(a) (b)

(c) (d)

Fig. 2. The 2-D profiles of (a) n_e, (b) T_e, (c) ϕ, (d) $E_{I\theta}$, (e) R_i, (f) q_J for a gas pressure 10 mTorr and power 500 W.

where J_{ew}, J_{iw} are the x-components of $\boldsymbol{J_e}$ and $\boldsymbol{J_i}$ to the wall, V_i is the Bohm velocity. The subscript s represents the position of the plasmas-sheath boundary.

For T_e, on the axis and side wall, $\partial T_e/\partial r = 0$; on the bottom $\partial T_e/\partial x = 0$; on the top $Q_{ew} = J_{ew}(2kT_{es} + e\Delta\phi)$.

The typical 2-D profiles for plasma density n_e, electron temperature T_e, plasma potential ϕ, the azimuthal electric field intensity $E_{I\theta}$, the ionization rate R_i and the plasma power deposition q_J are shown in Fig. 2. The total input power is 500 W, the neutral pressure is 10 mTorr. The amplitude of coil current is 39 A, the maximum plasma density is 3.36×10^{11} cm^{-3}, the maximum plasma potential is 15.1 V and the maximum electron temperature is about 3.9 eV. These results seem quite close to those obtained experimentally in [11], n_e is about 3.75×10^{11} cm^{-3}, ϕ is about 16 V and T_e is about 3.7 eV. The inductive electric field decreases rapidly from the roof to the bulk plasma due to the finite skin depth (about 1–2 cm for 10^{11}–10^{12} cm^{-3} plasma density). The contours of the azimuthal electric field in the reactor are also presented in Fig. 3. Its spatial distribution shape seems consistent with the published measurements [10] and the computional results in [17]. In Fig. 2(f), the peak power deposition is near the upper surface, and most of the energy was absorbed by the plasma within the skin layer in this region. It can also be seen that the peak plasma density is off axis. Near the bottom of the chamber, at large radius (greater than

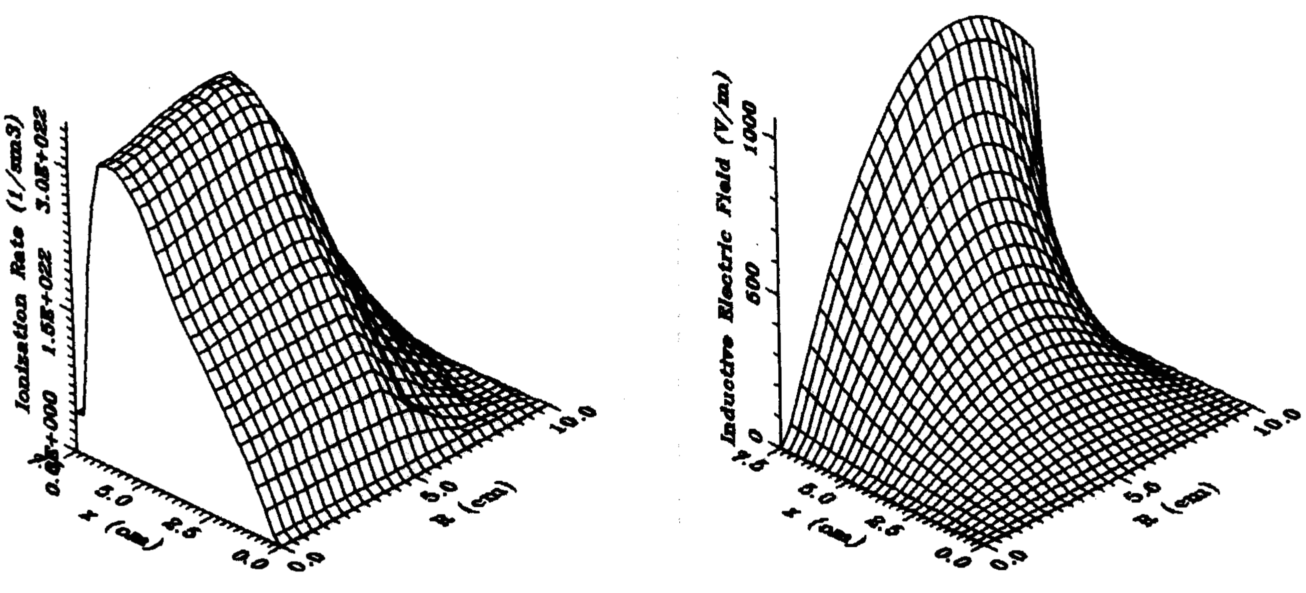

(e)

(f)

Fig. 2. (*Continued.*)

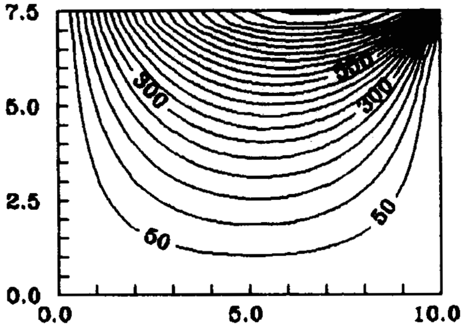

Fig. 3. The contours of the azimuthal electric field (V/m) in the reactor.

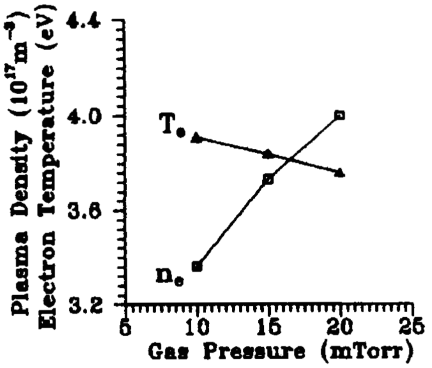

Fig. 4. The variations of n_e and T_e versus gas pressure for power 500 W.

8 cm), the plasma density has a good uniformity. In addition, the variation of the electron temperature in the chamber is not very large (less than 1 eV).

The effects of gas pressure and plasma power on the plasma characteristics were also studied. The variations of n_e and T_e with pressure and power are shown in Figs. 4 and 5, respectively. When the gas pressure increases from 10 mTorr to 20 mTorr, T_e decreases slightly, while n_e increases. When the power input increases, n_e increases linearly while T_e increases slightly. ϕ has the same variation trend as T_e with

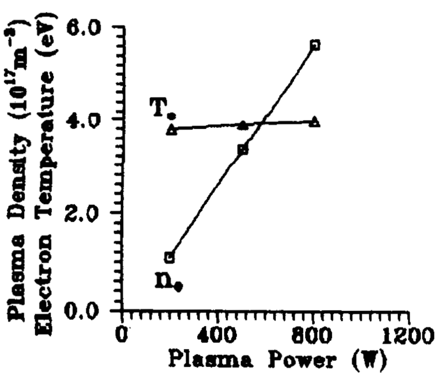

Fig. 5. The variations of n_e and T_e versus the input power for gas pressure 10 mTorr.

the pressure and power input and ϕ is about 3.9 T_e. These trends are in accord with our previous estimates [14] and experimental results [11].

ACKNOWLEDGMENT

The authors gratefully acknowledge the constructive suggestions made by Prof. D. B. Graves in the Department of Chemical Engineering, University of California at Berkeley. M. Li thanks Dr. U. Schmidt from the University of California at Berkeley for giving much help in the revised paper.

REFERENCES

[1] M. A. Lieberman and R. A. Gottscho, "Design of high density plasma sources for materials processing," in *Physics of Thin Films*, M. Francombe and J. Vossen, Eds. New York: Academic, 1993.

[2] D. B. Graves, "Plasma processing," *IEEE Trans. Plasma Sci.*, vol. 22, pp. 31–42, Feb. 1994.

[3] Y. Weng and M. J. Kushner, "Electron energy distribution in electron cyclotron resonance discharges for material processing," *J. Appl. Phys.*, vol. 72, pp. 33–42, 1992.

[4] C. K. Birdsall, "Particle-in-cell charged-particle simulations, plus Monte Carlo collisions with neutral atoms, PIC-MCC," *IEEE Trans. Plasma Sci.*, vol. 19, pp. 65–85, Feb. 1992.

[5] R. K. Porteous, H. M. Wu, and D. B. Graves, "A two-dimensional axisymmetric model of a magnetized glow discharge plasma," *Plasma Sources Sci. Technol.*, vol. 3, p. 25, 1994.

[6] N. Sato, S. Iizuka, Y. Nakagawa, and T. Tsukada, "Uniform plasma produced by a plane slotted antenna with magnets for electron cyclotron resonance," *Appl. Phys. Lett.*, vol. 62, pp. 1469–1471, 1993.

[7] D. B. Graves, H. Wu, and R. K. Porteous, "Modeling and simulation of high density plasma," *Japan. J. Appl. Phys.*, vol. 32, pp. 2999–3006, 1993.

[8] J. A. O'Neill, M. S. Barnes, and J. H. Keller, "Option ion energy measurement in a radio-frequency-induction plasma source," *J. Appl. Phys.*, vol. 73, pp. 1621–1626, 1993.

[9] M. S. Barnes, J. C. Forster, and J. H. Keller, "Electron energy distribution function measurement in a planar inductive oxygen radio frequency glow discharge," *Appl. Phys. Lett.*, vol. 62, pp. 2622–2624, 1993.

[10] J. Hopwood, C. R. Guarnieri, S. J. Whitehair, and J. J. Cuomo, "Electromagnetic fields in a radio-frequency induction plasma," *J. Vac. Sci. Technol. A*, vol. 11, pp. 147–151, 1993.

[11] ——, "Langmuir probe measurements of a radio frequency induction plasma," *J. Vac. Sci. Technol. A*, vol. 11, pp. 152–156, 1993.

[12] J. Hopwood, "Ion bombardment energy distributions in a radio frequency induction plasma," *Appl. Phys. Lett.*, vol. 62, pp. 940–942, 1993.

[13] A. E. Wendt, L. J. Mahoney, and J. L. Shohet, presented at the 45th Gaseous Electron. Conf., Boston, MA, 1992, paper LB-5, unpublished.

[14] H. Wu, L. Ming, and C. Yunming, and C. K. Wu, "Estimation of parameters of ICP source with a global model," *Chinese Phys, Lett.*, vol. 12, pp. 281–284, 1994.

[15] R. A. Stewart, P. Vitello, and D. B. Graves, "Two-dimensional fluid model of high density inductively coupled plasma sources," *J. Vac. Sci. Technol. B*, vol. 12, pp. 478–485, 1994.

[16] P. L. G. Ventzek, R. J. Hoekstra, T. J. Sommerer, and M. J. Kushner, "Two-dimensional hybrid model of induetively coupled plasma sources for etching," *Appl. Phys. Lett.*, vol. 63, pp. 605–607, 1993.

[17] P. L. G. Ventzek, R. J. Hoekstra, and M. J. Kushner, "Two-dimensional modeling of high plasma density inductively coupled sources for materials processing," *J. Vac. Sci. Technol. B*, vol. 12, pp. 461–477, 1994.

[18] X. Chen and E. Pfender, "Modeling of RF plasma torch with a metallic tube inserted for reactant injection," *Plasma Chem. Plasma Processing*, vol. 11, pp. 103–128, 1991.

[19] B. W. Yu and S. L. Girschick, "Modeling inductively coupled plasmas: The coil current boundary conditions," *J. Appl. Phys.*, vol. 69, pp. 656–661, 1991.

Ming Li was born in Henan, China, in 1967. He received the B.S. degree from Beijing University of Aeronautics and Astronautics, and the M.S. degree in fluid dynamics from the Institute of Mechanics, Chinese Academy of Sciences, in 1988 and 1991, respectively.

Since he joined the plasma division of the Institute of Mechanics in 1991, he has engaged in the numerical simulations of plasma and the study on particle-plasma interaction. In February 1995, he joined the Department of Chemical Engineering, University of California at Berkeley as a Visiting Researcher, and now he is carrying on the research of high density plasma models and simulations.

Han-Ming Wu was born in Shanghai, China, on July 2, 1952.

He is a Ph.D. Research Professor with the Institute of Mechanics, Chinese Academy of Sciences. He has been interested in plasma assisted material processing research work, such as inductively coupled plasma (ICP) research both in theoretical and experimental areas. Under the cooperation with the Research and Development Center of Microelectronics, Chinese Academy of Sciences, he has initiated the submicrometer etching processing research project.

Yunming Chen was born in Shanghai, China in 1937. He received the B.S. degree from Peking University and the M.S. degree in fluidmechanics from the Institute of Mechanics, Chinese Academy of Sciences, in 1960 and 1966, respectively.

From 1968 to 1980, he visited and joined the research project on the injection molding of polymers at Cornell University, Ithaca, NY. His current research interests include thermal plasma generation and applications in the preparation of ultrafine ceramic powders. He is a Professor in the Institute of Mechanics, Chinese Academy of Sciences, and a standing member of the Editorial Board of *Acta Mechanica Sinica*.